

Phosphatidylcholine contributes to *in vivo* ^{31}P MRS signal from the human liver

Marek Chmelík · Ladislav Valkovič · Peter Wolf · Wolfgang Bogner · Martin Gajdošák · Emina Halilbasic · Stephan Gruber · Michael Trauner · Michael Krebs · Siegfried Trattnig · Martin Kršák

Received: 5 September 2014 / Revised: 13 November 2014 / Accepted: 18 December 2014 / Published online: 11 January 2015
© European Society of Radiology 2015

Abstract

Objectives To demonstrate the overlap of the hepatic and bile phosphorus (^{31}P) magnetic resonance (MR) spectra and provide evidence of phosphatidylcholine (PtdC) contribution to the *in vivo* hepatic ^{31}P MRS phosphodiester (PDE) signal, suggested in previous reports to be phosphoenolpyruvate (PEP).

Methods Phantom measurements to assess the chemical shifts of PEP and PtdC signals were performed at 7 T. A retrospective analysis of hepatic 3D ^{31}P MR spectroscopic imaging (MRSI) data from 18 and five volunteers at 3 T and 7 T, respectively, was performed. Axial images were inspected for the presence of gallbladder, and PDE signals in representative spectra were quantified.

Results Phantom experiments demonstrated the strong pH-dependence of the PEP chemical shift and proved the overlap of PtdC and PEP (~2 ppm relative to phosphocreatine) at hepatic pH. Gallbladder was covered in seven of 23 *in vivo* 3D-MRSI datasets. The $\text{PDE}_{\text{gall}}/\gamma\text{-ATP}_{\text{liver}}$ ratio was 4.8-fold higher ($p=0.001$) in the gallbladder ($\text{PDE}_{\text{gall}}/\gamma\text{-ATP}_{\text{liver}}=3.61$

± 0.79) than in the liver ($\text{PDE}_{\text{liver}}/\gamma\text{-ATP}_{\text{liver}}=0.75\pm 0.15$). *In vivo* 7 T ^{31}P MRSI allowed good separation of PDE components. The gallbladder is a strong source of contamination in adjacent ^{31}P MR hepatic spectra due to biliary phosphatidylcholine.

Conclusions *In vivo* ^{31}P MR hepatic signal at 2.06 ppm may represent both phosphatidylcholine and phosphoenolpyruvate, with a higher phosphatidylcholine contribution due to its higher concentration.

Key Points

- *In vivo* ^{31}P MRS from the gallbladder shows a dominant biliary phosphatidylcholine signal at 2.06 ppm.
- *Intrahepatic* ^{31}P MRS signal at 2.06 ppm may represent both intrahepatic phosphatidylcholine and phosphoenolpyruvate.
- *In vivo* ^{31}P MRS has the potential to monitor hepatic phosphatidylcholine.

Keywords Liver · Phosphatidylcholine · Gallbladder · *In vivo* ^{31}P magnetic resonance spectroscopy · 7 Tesla,

Abbreviations

PtdC	phosphatidylcholine
PCr	phosphocreatine
PDE	phosphodiesters
PEP	phosphoenolpyruvate
Pi	inorganic phosphate
PME	phosphomonoesters
AMARES	advanced method for accurate, robust and efficient spectral fitting
B_0	magnetic field strength
MRSI	magnetic resonance spectroscopic imaging
GPC	glycerol 3-phosphorylcholine
GPE	glycerol 3-phosphorylethanolamine
MRS	magnetic resonance spectroscopy
^{31}P	phosphorus
TE	echo time

M. Chmelík · L. Valkovič · W. Bogner · M. Gajdošák · S. Gruber · S. Trattnig · M. Kršák (✉)
MR Centre of Excellence, Department of Biomedical Imaging and Image-guided Therapy, Medical University of Vienna, Vienna, Austria
e-mail: martin.krssak@meduniwien.ac.at

L. Valkovič
Department of Imaging Methods, Institute of Measurement Science, Slovak Academy of Sciences, Bratislava, Slovakia

P. Wolf · M. Krebs · M. Kršák
Division of Endocrinology and Metabolism, Department of Internal Medicine III, Medical University of Vienna, Vienna, Austria

E. Halilbasic · M. Trauner
Division of Gastroenterology and Hepatology, Department of Internal Medicine III, Medical University of Vienna, Vienna, Austria

TR	repetition time
FWHM	full width at half maximum
SD	standard deviation

Introduction

In vivo phosphorus (^{31}P) magnetic resonance spectroscopy (MRS) provides unique non-invasive information about human liver metabolism under various physiological and pathological conditions [1–9]. Alterations of cell membrane precursors (phosphomonoesters [PME]) and cell membrane degradation product (phosphodiesters [PDE]) levels have been associated with alcoholic, viral, and cholestatic aetiologies, regenerative changes, alcoholic and nonalcoholic fatty liver disease, cirrhosis, diabetes, or liver metastases [2–6, 10].

In addition, in vitro ^{31}P MRS enables quantitation of tissue phospholipids [11, 12]. Several in vitro and in vivo ^{31}P MRS studies of human bile [12–15] and liver tissue extracts [12, 16] showed a dominant peak of phosphatidylcholine (PtdC), a typical phosphodiester and part of bile lecithin [17]. A high concentration of PtdC in the gallbladder was also previously visualized by in vivo ^1H single-voxel MRS [18]. PtdC is an essential phospholipid in mammalian cells and is produced in all nucleated cells and tissues via a choline pathway [19]. PtdC synthesis is essential for VLDL secretion from the liver [19]. Alterations in PtdC metabolism were directly linked with alcoholic [20] and nonalcoholic fatty liver disease [21], as well as with hepatic cancer [14].

A direct comparison of in vivo and in vitro ^{31}P MRS results with the literature is often hampered by the use of different peaks as a chemical shift reference and a certain mismatch in terminology. Typically, phosphocreatine (PCr) is used as the 0 ppm reference in in vivo ^{31}P MR spectra [1–9]. On the other hand, 85 % inorganic orthophosphoric acid is used as reference (0 ppm) for in vitro ^{31}P MRS experiments [11, 12]. This results in a ~2.9 ppm difference in chemical shifts between in vitro and in vivo ^{31}P MRS spectra. All ^{31}P chemical shifts reported in this paper are relative to PCr ($\delta_{\text{PCr}}=0$ ppm). A terminological mismatch is mostly visible in the use of the PC abbreviation for phosphocholine for in vivo ^{31}P MR spectra or phosphatidylcholine in the in vitro ^{31}P MRS community. Alternative abbreviations for phosphatidylcholine (PtdC; PtdCho) have also been suggested [15, 22].

The main contributors to the in vivo hepatic ^{31}P MRS PDE signal are glycerophosphocholine (GPC) at 2.76 ppm and glycerophosphoethanolamine (GPE) at the 3.2 ppm resonance. The improvement of in vivo ^{31}P MRS resolution by proton broadband decoupling at lower magnetic fields (e.g., ≤ 3 T) [3, 7, 23], or by the application of ultra-high fields (e.g., ≥ 7 T) [22], allows for differentiation of these two metabolites and offers the ability to recognize an additional metabolic resonance at 2.06 ppm $_{\text{PCr}=0\text{ppm}}$ [3, 7, 22, 23]. Studies on cell

cultures and extracted liver biopsies assigned this resonance to phosphoenolpyruvate (PEP) [24] or perchloric acid extraction artefacts [8, 25]. Some of the literature about in vivo hepatic research adopted this assignment [3, 7, 23, 26]. It has been previously suggested that there was an overlap of PEP and PtdC in hepatic ^{31}P MRS spectra, but no evidence was provided [7, 22]. Pollesello et al. performed phantom measurements of mixed ^{31}P solutions [27], including PEP (2.45 ppm), but PtdC was missing. To the best of our knowledge, the only systematic MRS study that included both solutions was performed under alkaline conditions (e.g., pH=14) [28]. The chemical shift of PtdC is pH-independent [11]. Although a PEP chemical shift could be affected by pH, we are not aware of any systematic measurement in this respect. Both PEP and PtdC are potential important targets of metabolic research, and their contribution to the resonance at 2.06 ppm is a subject of current discussion [7, 13].

The importance of PEP is based on its highest-energy phosphate bond (-61.9 kJ/mol) and the involvement in both glycolysis and gluconeogenesis. The conversion of PEP to ADP by pyruvate-kinase generates one molecule of pyruvate and one molecule of ATP. Reversed phosphorylation of pyruvate to PEP by phosphoenolpyruvate-carboxykinase is considered to be a rate-limiting step in gluconeogenesis [29].

PtdC is the major component of biological membranes in addition to lecithin solutions. PtdC is a predominant phospholipid component of bile, protecting the bile ducts from the harmful effects of bile acids by the formation of mixed micelles [17]. A substantial part of PtdC is also secreted to the hepatic plasma where it contributes to plasmatic lipoproteins [19]. Thus, the in vivo assessment of biliary and hepatic PtdC is of potential diagnostic value in bile duct and liver disorders, where its impaired secretion may play a key role in the pathogenesis of these disorders [14, 20, 21, 30]. Moreover, PtdC may be a potential marker for the evaluation of the therapeutic efficacy of pharmacological biliary PtdC excretion enhancement [31].

The purpose of this study was to assess the overlap of the chemical shifts of PEP with PtdC in test solutions, taking the potential pH-dependence of the PEP resonance position into account. Further on, we aimed to assess the possible contribution of PtdC to the hepatic and biliary in vivo ^{31}P MRS signal at 2.06 ppm through retrospective quantification of in vivo ^{31}P 3D magnetic resonance spectroscopic imaging (MRSI) measurements of the hepatic region.

Materials and methods

Study design and volunteers

Institutional review board approval for ^{31}P MRSI measurements was obtained, and all subjects gave written informed

consent. In this retrospective study, data were analyzed from a total of 23 healthy volunteers ($m/f=14/9$; age= 40.4 ± 17.7 years; $BMI=24 \pm 3$ kg/m 2) who underwent liver ^{31}P MRSI in our institution between 2007 and 2009 at 3 T, and between 2011 and 2012 at 7 T. Healthy volunteers measured at 3 T represented a control group from a previous study of type II diabetes mellitus patients. Data from that study, in which hepatic tissue was studied exclusively, were published previously [4].

Data acquisition

Phantom experiments

In order to determine chemical shifts (i.e., signal positions in the ^{31}P MR spectrum), nine cylindrical test tubes ($\varnothing=2$ –2.5 cm, $V=10$ –20 ml) were filled with the following chemicals (Sigma Aldrich): inorganic phosphate ($\text{Pi}_{\text{pH}=7}$), phosphocreatine ($\text{PCr}_{\text{pH}=7}$), and $\text{PtdC}_{\text{pH}=7}$ (diluted in 40 % ethanol solution); and five PEP tubes with pH of 3, 5.5, 7, 12.3, and 14 (electronic pH tester reading). In addition, a human bile sample, acquired by biopsy during gallbladder surgery, was included. The pH of hepatic and gallbladder bile in humans ranges from 6.5 to 8 [32]. Tubes were placed in a plastic box filled with a physiological solution. Global magnetic field homogeneity across all tubes assessed by the FWHM of the water signal was ~10 Hz. Thus, susceptibility effects on the resonance position could be neglected. A 2D MRS imaging (MRSI) acquisition (32×32 , $TR=10$ s, $TA=3$ h) of the phantom object was acquired on a human 7 T MR system (Siemens, Healthcare, Erlangen, Germany) using a double-tuned surface coil ($^1\text{H}/^{31}\text{P}$, 298/120.7 MHz, $\varnothing=10$ cm, RAPID Biomedical GmbH, Rimpar, Germany).

In vivo experiments All measurements were performed in the morning after a 12-h overnight fast. Subjects were examined in the prone position with a 10-cm-diameter linearly polarized, double-tuned $^1\text{H}/^{31}\text{P}$ surface coil positioned under the lateral aspect of the liver on a 3 T ($n=18$) whole-body scanner (Medspec S30/80; Bruker Biospin, Ettlingen, Germany), or on a 7 T ($n=5$) MR system (Siemens Healthcare, Erlangen, Germany). This positioning was chosen to reduce breathing-related artefacts as much as possible. Axial MRI gradient-echo images (15 slices, $FOV=20 \times 20$ cm, 128×96 , $TE=3.4$ ms, $TR=120$ ms) covering the region of interest were acquired during one breath-hold, immediately before the ^{31}P MRSI scan (Figs. 2a and 3a). During the ^{31}P MRSI measurements, the subjects were instructed to breathe freely. The ^{31}P 3D k-space-weighted MRSI localization technique ($13 \times 13 \times 13$ matrix at 3 T or $12 \times 12 \times 12$ matrix at 7 T; field of view: $20 \times 20 \times 20$ cm 3 ; repetition time 1 s at 3 T, or 1.5 s at 7 T), with an adiabatic B_1 -insensitive, half-passage excitation pulse (2.5-ms sin/cos-modulated, bandwidth=4300 Hz) was used to acquire

^{31}P MR spectra. The whole protocol, including set-up, took approximately 45 min at 3 T and 21 min at 7 T.

Data processing Axial MR images were inspected for the presence of gallbladder signal. In all MRSI data sets, the matrix size was interpolated to $16 \times 16 \times 16$ voxels. The interpolated voxel size was $12.5 \times 12.5 \times 12.5$ mm 3 . Two representative spectra from each volunteer, one from gallbladder and one from liver tissue, at a similar distance from the centre of the coil, were selected for quantification. The AMARES time-domain-fitting algorithm was used to evaluate PDE signals in the selected spectra. In addition, the $\text{PtdC}+\text{PEP}/\gamma\text{-ATP}$ ratio was evaluated in nine voxels containing liver tissue at a minimum of 5 cm away from the gallbladder in each of the 7 T volunteers. Resonance positions in all ^{31}P MR spectra were referenced to the resonance of phosphocreatine ($\delta_{\text{PCr}}=0$ ppm).

Statistical methods

The mean and standard deviation (SD) of PDE integrals were computed for representative spectra from the gallbladder and liver. Both integrals were normalized to the $\gamma\text{-ATP}$ signal in liver tissue. To assess the difference between these two sets of data, we performed a two-tailed, paired t test. In addition, 3 T and 7 T results of both PDE/ $\gamma\text{-ATP}$, in the liver and gallbladder, were compared by an unpaired t-test. A $p\text{-value} \leq .05$ indicated a significant result.

Results

Phantom experiments

The results of the phantom experiments are summarized and depicted in Fig. 1. Localized spectra allowed precise assessment of metabolite chemical shifts. The following chemical shifts were observed: PCr (0 ppm), Pi (4.7 ppm), $\text{PEP}_{\text{pH}=3}$ (-1.2 ppm), $\text{PEP}_{\text{pH}=5.5}$ (-1 ppm), $\text{PEP}_{\text{pH}=7}$ (1.6 ppm), $\text{PEP}_{\text{pH}=12.3}$ (2.3 ppm), $\text{PEP}_{\text{pH}=14}$ (2.5 ppm), PtdC (2 ppm), and human bile (2 ppm). These results demonstrated the strong dependence of the PEP resonance position on pH, which is summarized in Fig. 1D. PtdC solution resonated at the same position as the dominant signal from the human bile sample. The PtdC solution showed two components due to the use of only ~60 % purified L- α -phosphatidylcholine from egg yolk. The second component may correspond to lysophosphatidylcholine, which is present in egg yolk [16], and its resonance was shifted ~0.7 ppm downfield from the PtdC resonance.

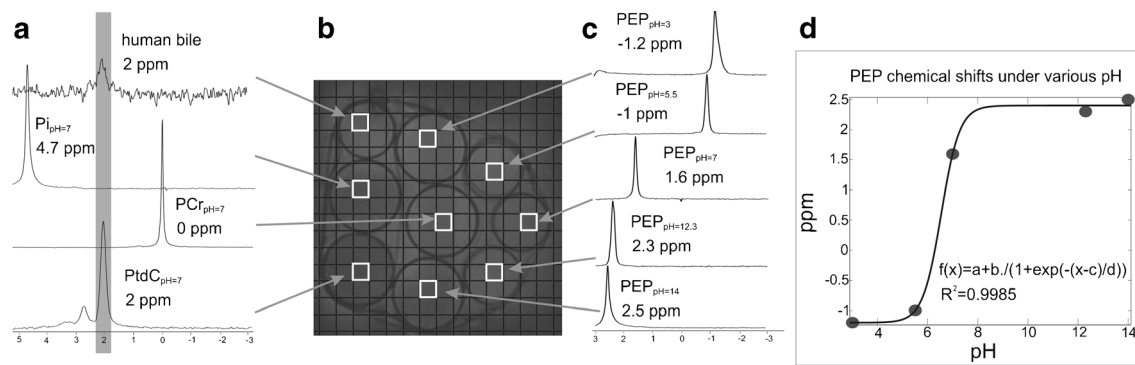


Fig. 1 Phantom measurements including nine samples (*B*) filled with Pi, PCr, 5× PEP (pH=3, 5.5, 7, 12.3, 14), PtdC, and human bile. Representative spectra of Pi, PCr, PtdC, and bile (*panel A*), as well as

PEP (*panel C*) are depicted. Note the strong dependence of the PEP chemical shift on the pH, summarized in graph *D*. The data points were fitted with a sigmoidal function.

In vivo results

Seven of 23 in vivo data sets included signal from the gallbladder. Figs. 2 and 3 show typical 3 T and 7 T MRS data, where both gallbladder and liver tissue were present in the acquired ³¹P 3D-MRSI data sets. A strong signal, resonating at approximately 2 ppm, was always detectable in the gallbladder. In addition, 7 T MRS data (Fig. 3) allowed good separation of PDE components, with a dominant signal at 2.06 ppm clearly resolved (Fig. 3C). Note also the contamination in liver tissue spectra adjacent to the gallbladder. The PDE/γ-ATP_{liver} ratio was, on average, 4.8-fold higher ($p=0.001$) in the gallbladder spectra (PDE_{gall}/γ-ATP_{liver}=3.61±0.79) than in the liver tissue (PDE_{liver}/γ-ATP_{liver}=0.75±0.15). No statistical difference was found between 3 T and 7 T PDE/ATP ratios, neither in hepatic tissue nor in gallbladder. Typical transversal slice from a 7 T in vivo ³¹P 3D MRSI dataset without gallbladder contamination is depicted in Fig. 4. The

PtdC+PEP/γ-ATP ratio in the non-contaminated liver tissue of the volunteers scanned at 7 T was 0.15 ± 0.05 .

Discussion

In our study, phantom measurements and a retrospective analysis of in vivo data showed that phosphatidylcholine (PtdC) contributes to the in vivo ³¹P MRS signal at 2.06 ppm, and is the dominant component in human bile MRS signal. The high in vivo concentration of PtdC in the gallbladder is in accordance with previous ¹H single-voxel MRS [18]. The observed PtdC chemical shift overlaps with the PEP resonance at physiological pH.

In vivo, the hepatic resonance at 2 ppm was previously assigned to phosphoenolpyruvate (PEP) [3, 23, 26] or to the effect of perchloric acid extraction [8, 25]. Evidence that confirmed the assignment of the PEP resonance position in

Fig. 2 This figure depicts a typical transversal slice from a 3 T in vivo ³¹P 3D MRSI dataset (*A*). Sample muscle (*B*), liver (*C-bottom*), and gallbladder (*C-top*) spectra are depicted. The quality of localization is reflected by the PCr resonance that is present in the muscle and lacking in the liver. Note the strong signal of phosphatidylcholine (PtdC) at 2 ppm in the gallbladder and its surrounding area (*C*).

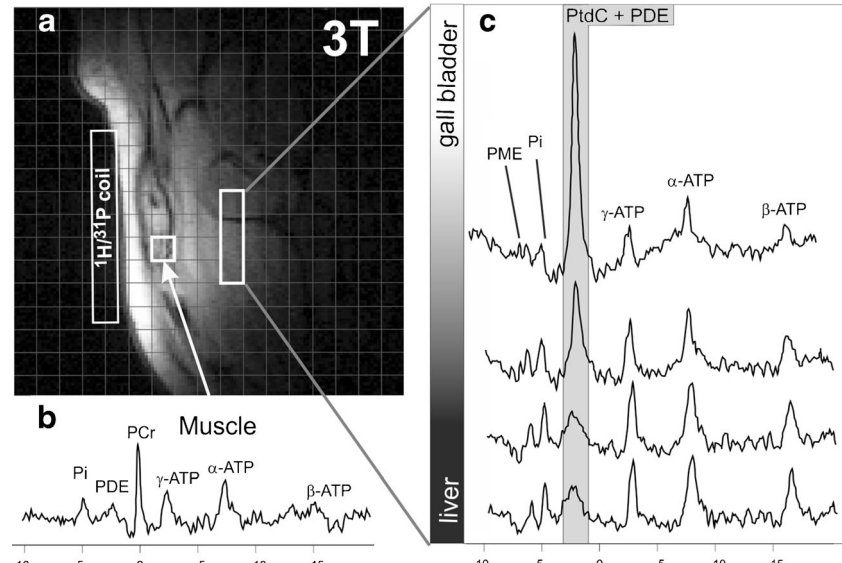
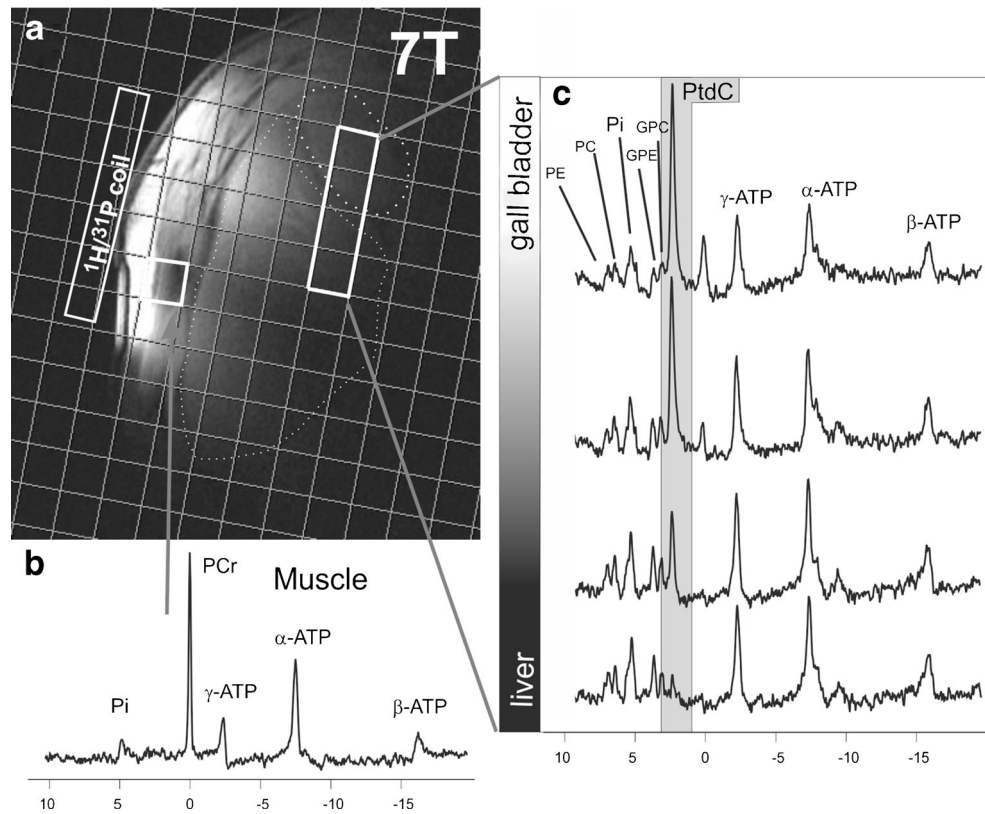


Fig. 3 Display of typical transversal slice from a 7 T *in vivo* ^{31}P 3D MRSI dataset (*A*). Sample muscle (*B*), liver (*C-bottom*), and gallbladder (*C-top*) spectra are depicted. The quality of localization is reflected by the PCr resonance that is present in the muscle and lacking in the liver. Note the strong signal of phosphatidylcholine (PtdC) at 2 ppm in the gallbladder and its surrounding area (*C*).

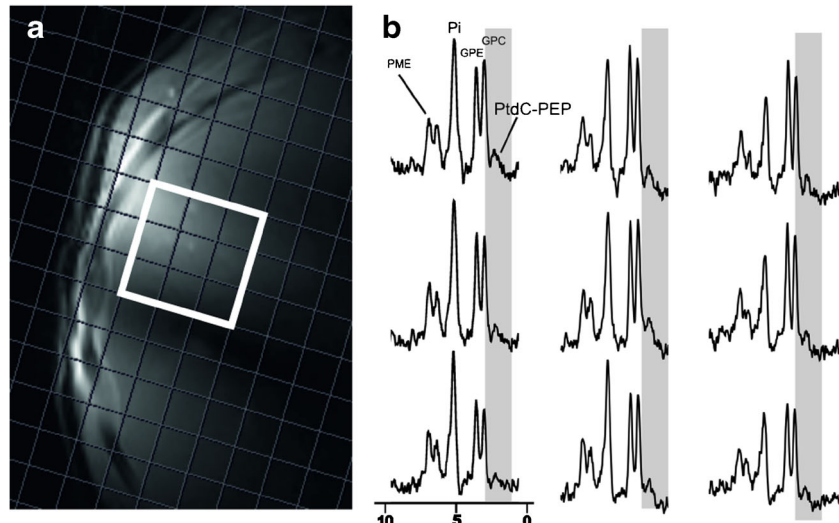


phantom solution measurements was provided under alkaline conditions (e.g., pH=14), which could have affected the chemical shift of PEP [28]. This was confirmed by our phantom experiment where the chemical shift of the PEP resonance showed a pH-dependence, with a downfield chemical shift (e.g., ~1.6 ppm) at a pH of 7. Other phantom measurements (pH~8) performed on mixture solutions, including PEP and a variety of other ^{31}P metabolites, showed the PEP resonance at 2.45 ppm [27]. These different chemical shifts may be partially explained by the strong sensitivity of the PEP chemical shift

to pH in the 6 – 9 range, as shown in our phantom experiment (Fig 1D).

The assessment of tissue PEP and PtdC concentrations could provide another clue to the proper assignment of resonance lines or for the estimation of their relative contribution to these lines in *in vivo* conditions. The *in vivo* concentration of the hepatic PEP was reported to be ~0.02 mmol/l [33], which would be below the detection limit for *in vivo* ^{31}P MRS. Hamasaki et al. detected the ^{31}P MRS signal of PEP in intact erythrocytes only after the addition of a high

Fig. 4 Display of typical transversal slice from a 7 T *in vivo* ^{31}P 3D MRSI dataset without gallbladder contamination (*A*). Downfield parts of sample liver (*B*) spectra are depicted. Note the signal of intrahepatic phosphatidylcholine (PtdC) and phosphoenolpyruvate (PEP) at 2 ppm.



concentration of PEP (65 mM) and toxic inhibition of glycolysis by sodium fluoride NaF. Non-toxic conditions resulted in immediate metabolism of PEP [34]. Further studies also showed the need for strong metabolic perturbation to increase the ^{31}P MRS signal of PEP. Stimulation of gluconeogenesis [35] or inhibition of glycolysis [27] were used for this purpose.

Although there is no information about intra-hepatic physiological *in vivo* PtdC concentrations, they could be estimated indirectly. Human bile consists of ~7 mmol/l of soluble phospholipids [36] and the majority (~50 %) consists of PtdC [12]. Considering an intrahepatic bile volume of ~29 ml (including micro and macro ducts [37]) and a hepatic tissue volume of ~1,500 ml results in an intra-hepatic PtdC concentration of ~0.07 mmol/l, which is approximately 3.5-times higher than the expected PEP concentration. PtdC+PEP/ATP ratio from this study (0.15 ± 0.05) and assumption of 2.14 mmol/l concentration of the hepatic ATP [38] would result in an estimated PtdC+PEP concentration of 0.32 ± 0.1 mmol/l (no T_1 relaxation times correction), which may reflect not only biliary, but also hepatic PtdC secreted to the plasma [19].

Our results also show that bile in the gallbladder is a strong source of MR signal contamination of hepatic spectra in the PDE region. This was already noted by Cox et al. [6], but, unfortunately, due to the lower spectral resolution at 1.6 T it was not possible to characterize which of the PDE was responsible for the contamination. To our knowledge, this strong source of contamination has not been discussed elsewhere. This signal contamination should be considered, particularly when using phase-encoding within MRSI measurement schemes with a small number of phase-encoding steps (typically the case in ^{31}P MRSI). In order to improve the point-spread function and reduce voxel bleeding, we used higher matrix sizes ($13 \times 13 \times 13$ at 3 T and $12 \times 12 \times 12$ at 7 T) in combination with weighted acquisition. Nevertheless, spectra from liver tissue, located two columns apart from the gallbladder, should still be considered contaminated by the bile signal. This contamination reflects an imperfect point-spread function—a typical localization error of the phase-encoding scheme used in MRSI experiments with a low number of phase-encoding steps. These artefacts are even more prominent in studies where lower phase-encoding matrices were used (e.g., 1×4 MRSI [39]; 1×8 MRSI [5]; 8×8 MRSI [23]). Such acquisition schemes could be prone to contamination by gallbladder bile due to imperfect localization.

Other localization schemes often used for ^{31}P MRS of the liver (e.g., 1D-ISIS, DRESS, or 3D-ISIS) use relatively large volumes and/or are prone to artefacts due to breathing motion. In such cases, the acquisition volume must be prescribed with exceptional care to avoid gallbladder from the volume of interest (VOI). Solanky et al [40] observed elevated PDEs

when biliary hyperplasia was present in the rat liver. Therefore, possible contamination should also be considered in patients with dilated intrahepatic bile ducts, for different reasons.

Another sign of possible contamination in the liver spectra by PtdC are high variations of previously reported absolute concentrations and T_1 relaxation times of PDEs [39]. Possible partial volume effects, as well as T_1 differences between PtdC and GPC+GPE, could partly explain these results. Future examinations aiming at bile PtdC would be necessary to explain its possible role in these variations. Furthermore, findings of altered hepatic PDE signals, especially when not ideally resolved, should be considered indicative of possible MRS contamination by hepatic bile or by gallbladder signals.

Detection of the gallbladder PtdC resonance in only seven ^{31}P MRS data sets was caused by the limited penetration of the surface coil, which did not allow for the localization of the gallbladder in all subjects. A coil with optimized geometry [41] in a dedicated experimental set-up should enable coverage of both the larger part of the liver and the gallbladder. The assessment of the absolute concentrations of the PtdC signal at $2.06 \text{ ppm}_{\text{PCr}=0\text{ppm}}$ in our study was hampered by a lack of knowledge of the T_1 relaxation time of PtdC at both field strengths, resulting in unpredictable partial saturation effects.

Further studies should investigate the potential use of the PtdC resonance for metabolic studies of the liver, gallbladder, and bile ducts. Changes in biliary PtdC may be indicator of malignancy and dynamic metabolic perturbation, representing cell breakdown, death, and cellular regeneration [14]. Notably, hereditary and acquired defects in biliary phosphatidylcholine secretion may play a key role in the pathogenesis of bile duct and liver diseases [14, 20, 21, 30], and the assessment of biliary PtdC could have diagnostic value in such disorders [14]. Moreover, pharmacological stimulation of biliary PtdC excretion, and its possible monitoring by ^{31}P MRS, may represent an interesting therapeutic approach to hepatobiliary disorders, and the use of several drugs (e.g., fibrates, ursodeoxycholic acid), since these drugs have been shown to enhance PtdC in bile [31].

In conclusion, our *in vitro* data showed the dependence of the phosphoenolpyruvate chemical shift on pH and its potential overlap with the PtdC resonance in physiological conditions. Our *in vivo* data showed a dominant ^{31}P MRS resonance at 2.06 ppm in the gallbladder region that arose from biliary phosphatidylcholine, whereas we suggest that the ^{31}P MR hepatic signal at 2.06 ppm may represent both intrahepatic phosphatidylcholine and phosphoenolpyruvate with the major contribution from phosphatidylcholine due to its higher concentration. *In vivo* ^{31}P MRS has the potential to monitor noninvasively hepatic phosphatidylcholine and assess its concentration.

Acknowledgments We thank Vladimir Mlynarik for a helpful discussion. The scientific guarantor of this publication is Associate Professor Martin Kršák, Ph.D. The authors of this manuscript declare no relationships with any companies, whose products or services may be related to the subject matter of the article. This study was supported by the Vienna Spots of Excellence des Wiener Wissenschafts-und Technologie-Fonds (WWTF) – Vienna Advanced Imaging Center (VIACLIC), and the OeNB Jubiläumsfond (grants #13629, #15455, and #15363). No complex statistical methods were necessary for this paper. Institutional review board approval was obtained. Written informed consent was obtained from all subjects in this study. Some study subjects or cohorts have been previously reported in Szendoedi and Chmelik et al. (Hepatology, 2009). Methodology: prospective / retrospective, experimental, performed at one institution.

Parts of this study were presented at the ISMRM, 2013, Salt Lake City (Chmelik, M. et al., Human bile phosphatidylcholine contributes to ^{31}P MRS hepatic signal at 2.06 ppm. (e-poster ID#4090)).

References

- Menon DK, Sargentoni J, Taylor-Robinson SD et al (1995) Effect of functional grade and etiology on in vivo hepatic phosphorus-31 magnetic resonance spectroscopy in cirrhosis: biochemical basis of spectral appearances. *Hepatology* 21:417–427
- Taylor-Robinson SD, Sargentoni J, Bell JD et al (1997) In vivo and in vitro hepatic ^{31}P magnetic resonance spectroscopy and electron microscopy of the cirrhotic liver. *Liver* 17:198–209
- Sebastianova K, Hakkarainen A, Kotronen A et al (2010) Nonalcoholic fatty liver disease: detection of elevated nicotinamide adenine dinucleotide phosphate with in vivo 3.0-T (^{31}P) MR spectroscopy with proton decoupling. *Radiology* 256:466–473
- Szendoedi J, Chmelik M, Schmid AI et al (2009) Abnormal hepatic energy homeostasis in type 2 diabetes. *Hepatology* 50:1079–1086
- Taylor-Robinson SD, Sargentoni J, Bell JD et al (1998) In vivo and in vitro hepatic phosphorus-31 magnetic resonance spectroscopy and electron microscopy in chronic ductopenic rejection of human liver allografts. *Gut* 42:735–743
- Cox IJ, Sargentoni J, Calam J, Bryant DJ, Iles RA (1988) Four-dimensional phosphorus-31 chemical shift imaging of carcinoid metastases in the liver. *NMR Biomed* 1:56–60
- Wylezinska M, Cobbold JFL, Fitzpatrick J et al (2011) A comparison of single-voxel clinical in vivo hepatic (^{31}P) MR spectra acquired at 1.5 and 3.0 Tesla in health and diseased states. *NMR Biomed* 24:231–237
- Dagnelie PC, Bell JD, Cox IJ et al (1993) Effects of fish oil on phospholipid metabolism in human and rat liver studied by ^{31}P NMR spectroscopy in vivo and in vitro. *NMR Biomed* 6:157–162
- Valkovic L, Gajdosik M, Traussnigg S et al (2014) Application of localized (^{31}P) MRS saturation transfer at 7 T for measurement of ATP metabolism in the liver: reproducibility and initial clinical application in patients with non-alcoholic fatty liver disease. *Eur Radiol* 24:1602–1609
- Taylor-Robinson SD, Thomas EL, Sargentoni J, Marcus CD, Davidson BR, Bell JD (1995) Cirrhosis of the human liver: an in vitro ^{31}P nuclear magnetic resonance study. *Biochim Biophys Acta* 1272:113–118
- London E, Feigenson GW (1979) Phosphorus NMR analysis of phospholipids in detergents. *J Lipid Res* 20:408–412
- Metz KR, Dunphy LK (1996) Absolute quantitation of tissue phospholipids using ^{31}P NMR spectroscopy. *J Lipid Res* 37:2251–2265
- Ijare O, Bezabeh T, Albiin N, et al (2011) Potential of ^{31}P magnetic resonance spectroscopy of bile in the detection of cholestatic diseases, Proceedings of the 19th Annual Meeting ISMRM , Montreal, Canada, 2011; 1002
- Khan SA, Cox IJ, Thillainayagam AV, Bansal DS, Thomas HC, Taylor-Robinson SD (2005) Proton and phosphorus-31 nuclear magnetic resonance spectroscopy of human bile in hepatopancreaticobiliary cancer. *Eur J Gastroenterol Hepatol* 17:733–738
- Bala L, Tripathi P, Bhatt G et al (2009) (1)H and (31)P NMR studies indicate reduced bile constituents in patients with biliary obstruction and infection. *NMR Biomed* 22:220–228
- Sotirhos N, Hersløf B, Kenne L (1986) Quantitative analysis of phospholipids by ^{31}P -NMR. *J Lipid Res* 27:386–392
- Small DM, Bourges M, Dervichian DG (1966) Ternary and quaternary aqueous systems containing bile salt, lecithin, and cholesterol. *Nature* 211:816–818
- Prescot AP, Collins DJ, Leach MO, Dzik-Jurasz AS (2003) Human gallbladder bile: noninvasive investigation in vivo with single-voxel ^1H MR spectroscopy. *Radiology* 229:587–592
- Li Z, Vance DE (2008) Phosphatidylcholine and choline homeostasis. *J Lipid Res* 49:1187–1194
- Lieber CS (2004) New concepts of the pathogenesis of alcoholic liver disease lead to novel treatments. *Curr Gastroenterol Rep* 6:60–65
- Song J, da Costa KA, Fischer LM et al (2005) Polymorphism of the PEMT gene and susceptibility to nonalcoholic fatty liver disease (NAFLD). *Faseb J* 19:1266–1271
- Chmelik M, Povazan M, Krssak M et al (2014) In vivo (^{31}P) magnetic resonance spectroscopy of the human liver at 7 T: an initial experience. *NMR Biomed* 27:478–485
- Schlemmer HP, Sawatzki T, Sammet S et al (2005) Hepatic phospholipids in alcoholic liver disease assessed by proton-decoupled ^{31}P magnetic resonance spectroscopy. *J Hepatol* 42:752–759
- Ugurbil K, Rottenberg H, Glynn P, Shulman RG (1978) ^{31}P nuclear magnetic resonance studies of bioenergetics and glycolysis in anaerobic Escherichia coli cells. *Proc Natl Acad Sci U S A* 75:2244–2248
- Bell JD, Cox IJ, Sargentoni J et al (1993) A ^{31}P and ^1H -NMR investigation in vitro of normal and abnormal human liver. *Biochim Biophys Acta* 1225:71–77
- de Graaf RA (2007) In vivo NMR spectroscopy, 2nd edn. Wiley, West Sussex
- Pollello P, Eriksson O, Vittur F, Paoletti S, Geimonen E, Toffanin R (1995) Detection and quantitation of phosphorus metabolites in crude tissue extracts by ^1H and ^{31}P NMR: use of gradient assisted ^1H - ^{31}P HMQC experiments, with selective pulses, for the assignment of less abundant metabolites. *NMR Biomed* 8:190–196
- Turner BL, Mahieu N, Condron LM (2003) Phosphorus-31 nuclear magnetic resonance spectral assignments of phosphorus compounds in soil NaOH-EDTA extracts. *Soil Sci Soc Am J* 67:497–510
- Rognstad R (1979) Rate-limiting steps in metabolic pathways. *J Biol Chem* 254:1875–1878
- Trauner M, Fickert P, Wagner M (2007) MDR3 (ABCB4) defects: a paradigm for the genetics of adult cholestatic syndromes. *Semin Liver Dis* 27:77–98
- Halilbasic E, Claudel T, Trauner M (2013) Bile acid transporters and regulatory nuclear receptors in the liver and beyond. *J Hepatol* 58: 155–168
- Shiffman ML, Sugerman HJ, Moore EW (1990) Human gallbladder mucosal function. Effect of concentration and acidification of bile on cholesterol and calcium solubility. *Gastroenterology* 99:1452–1459
- Storey KB (2004) Functional metabolism: regulation and adaptation. Wiley, Hoboken
- Hamasaki N, Wyrwicz AM, Lubansky JH, Omachi A (1981) A ^{31}P NMR study of phosphoenolpyruvate transport across the human erythrocyte membrane. *Biochem Biophys Res Commun* 100:879–887
- Dagnelie PC, Menon DK, Cox IJ et al (1992) Effect of L-alanine infusion on ^{31}P nuclear magnetic resonance spectra of normal human

- liver: towards biochemical pathology *in vivo*. *Clin Sci (Lond)* 83: 183–190
36. Watson R, Preedy V (2013) Bioactive food as dietary interventions for liver and gastrointestinal disease. Elsevier
 37. Ludwig J, Ritman EL, LaRusso NF, Sheedy PF, Zumpe G (1998) Anatomy of the human biliary system studied by quantitative computer-aided three-dimensional imaging techniques. *Hepatology* 27:893–899
 38. Chmelik M, Schmid AI, Gruber S et al (2008) Three-dimensional high-resolution magnetic resonance spectroscopic imaging for absolute quantification of 31P metabolites in human liver. *Magn Reson Med* 60:796–802
 39. Sijens PE, Dagnelie PC, Halfwerk S, van Dijk P, Wicklow K, Oudkerk M (1998) Understanding the discrepancies between P-31 MR spectroscopy assessed liver metabolite concentrations from different institutions. *Magn Reson Imaging* 16:205–211
 40. Solanky BS, Sanchez-Canon GJ, Cobbold JF et al (2012) Metabolic profiling of the rat liver after chronic ingestion of alpha-naphthylisothiocyanate using *in vivo* and *ex vivo* magnetic resonance spectroscopy. *Toxicol Sci Off J Soc Toxic* 126: 306–316
 41. Panda A, Jones S, Stark H et al (2012) Phosphorus liver MRSI at 3 T using a novel dual-tuned eight-channel 31P/1H coil. *Magn Reson Med* 68:1346–1356